J Mar Sci Technol (2002) 7:79–85

Journal of
Marine Science
and Technology

Influence of microbubble diameter and distribution on frictional resistance reduction

Yasuhiro Moriguchi and Hiroharu Kato

Department of Mechanical Engineering, Toyo University, 2100 Kujirai, Kawagoe 350-8585, Japan

Abstract Investigations into frictional resistance reduction by microbubbles were carried out using a two-dimensional channel. The flow velocity and the amount of air injected were varied, and the frictional resistance reduction was measured. The frictional resistance reduction increased with increasing mean void ratio. When the bubble diameter was changed, the influence on frictional resistance reduction was negligible. The influence of bubble distribution near a wall was also investigated. Although it is thought that the influence of microbubbles near a wall is large, further investigations are required.

Key words Microbubble · Frictional resistance · Void ratio · Bubble diameter

List of symbols

- b breadth of test section (m)
- C_f local frictional resistance coefficient
- C_{fp} C_f derived from a pressure drop along the test section
- d bubble diameter (m)
- D diameter of the air injection hole (m)
- h height of test section (m)
- Q flow rate (m^3/s)
- U flow velocity (m/s)

Greek symbols

- α void ratio
- ρ density (kg/m^3)
- τ shearing stress (Pa)

Subscripts

- a air
- m mean
- 0 without microbubbles
- w wall, water

Address correspondence to: H. Kato (kato@eng.toyo.ac.jp)
Received: February 6, 2002 / Accepted: April 30, 2002

Introduction

Since the efficiency of a machine can be increased by reducing the frictional resistance, research on this subject has been carried out in various countries in the world. Methods such as the use of riblets, polymers, surface-active agents, and microbubbles have been examined as frictional resistance reduction devices. We have investigated whether microbubbles are suitable for reducing the frictional resistance of a vessel.

If many small bubbles (air bubbles, hydrogen bubbles, etc.) with a diameter of 0.2–2 mm exist in a boundary layer, the frictional resistance of a wall surface will decrease. McCormick and Bhattacharyya[1] identified this phenomenon in 1973. They generated microbubbles of hydrogen by electrolyzing water, and obtained a 10%–30% reduction in the frictional resistance. In this experiment, although the energy of the electrolysis was greater than the energy saved from the reduction in frictional resistance, the fundamental phenomenon was demonstrated and the effect was proved.

In 1977, Russian researchers found that frictional resistance decreased sharply with the use of microbubbles of air injected from a porous plate into a turbulent boundary layer.[2] Microbubbles of air were easy to generate at low cost and had little effect on the environment. The maximum reduction rate reached more than 80% (i.e., the resistance was one-fifth of the original value).

Although this rate of resistance reduction is high compared with other devices, the mechanism is not yet clear. Madavan et al.[3–5] conducted measurements and calculations of the local frictional resistance on a wall surface in turbulent flow to try to clarify the mechanism. Recently, Kato and co-workers[6–11] carried out experimental research on this subject. They measured velocity as well as turbulence intensity in a boundary layer filled with microbubbles.[10] The turbulence intensity increased

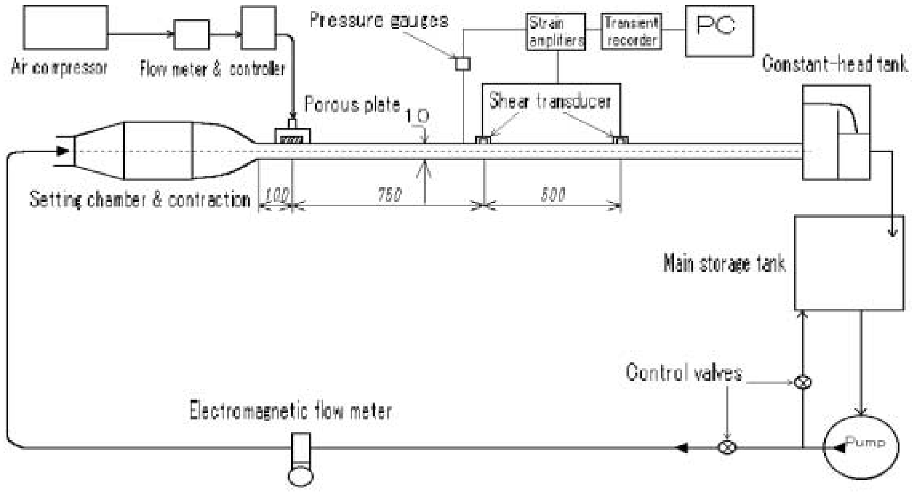

Fig. 1. Experimental equipment

at low microbubble density, and then began to decrease with increasing bubble density. These results indicate that the effect of microbubbles is complicated and requires further experimental investigation.

The endurance of the effect of microbubbles was tested using a long model ship, and aiming at the practical utilization of microbubbles.[12,13] Methods of generating the microbubbles were also investigated.[8,14]

The effect of microbubble diameter on the reduction of frictional resistance is another important issue to be resolved. This article is a report on experimental results concerning the effect of microbubble diameter and the distribution of microbubbles in the boundary layer. These experiments were aimed at understanding the mechanism of resistance reduction.

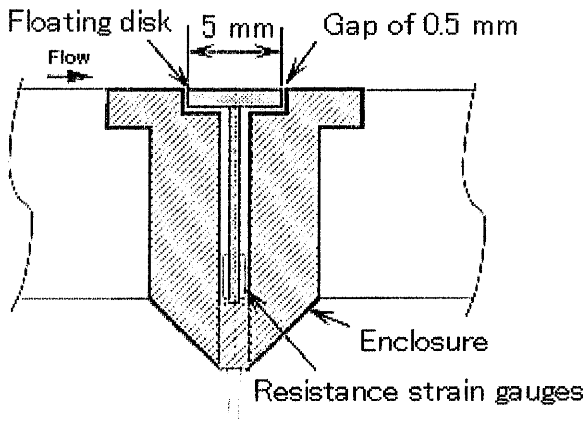

Fig. 2. Shear transducer

Experimental equipment

The experiment was conducted using the two-dimensional recirculating water channel shown in Fig. 1. The test section, which was 10mm high, 100mm wide, and 2000mm long, could easily generate a fully developed turbulent flow. An aspect ratio of 10 in the test section ensured a two-dimensional flow.

The flow was generated by a centrifugal pump, passed along an electromagnetic flow meter and through the settling chamber, and then entered the test section. Microbubbles were injected through a porous plate in the test section at the upstream upper surface, generating a gas–liquid flow.

Frictional resistance was measured by shear transducers set 750mm and 1250mm downstream of the air injection port. The shear transducers consisted of a floating disk with a diameter of 5mm supported by a cantilever plate, whose distortion was measured by two strain gauges, as shown in Fig. 2. The capacity of each transducer was only 1g. The pressure decrease along the test section was measured by pressure taps situated on the side wall. The measured data were processed by a strain meter and a transient recorder, and were analyzed with a personal computer.

The shear transducer was calibrated statically using a small weight. It was then calibrated dynamically in the channel. The dynamic calibration result was always substantially different from that of static calibration. This was because of the pressure force acting on the side wall of the floating disk. Detailed discussions are given later.

Experimental results

Measurement of the shear stress and pressure loss

First, the shear stress and pressure loss of the test section were measured in a flow without microbubbles to check the accuracy of the frictional resistance measurement. The experiment was performed at a flow velocity of 4–8 m/s, and an airflow rate of 0 l/min. The data obtained from the two shear transducers were analyzed and compared with those obtained by the pressure drop along the test section.

Figure 3 shows the relation between the frictional resistance coefficient measured directly by the shear transducers and those calculated from the pressure drop. Definitions of the mean flow velocity U_m and the frictional resistance coefficients C_f are given by Eqs. 1 and 2, respectively.

$$U_m = \frac{Q_a + Q_w}{b \cdot h} \tag{1}$$

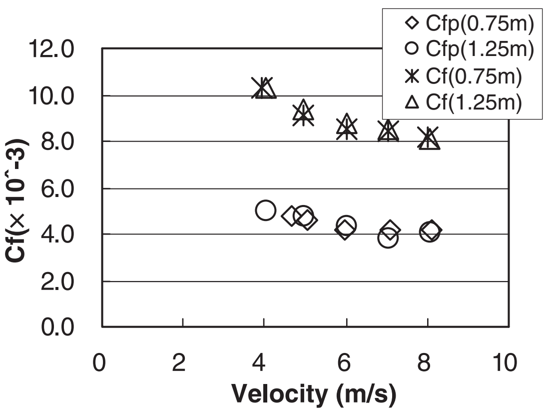

Fig. 3. Frictional resistance without microbubbles

$$C_f = \frac{\tau_w}{0.5 \cdot \rho \cdot U_m^2} \tag{2}$$

Although there is a difference between the frictional resistance (C_f) measured directly by the shear transducer and the frictional resistance (C_{fp}) calculated from the pressure drop, they are proportional to each other. Such a tendency is often obtained with this type of transducer. Guin et al.[7] examined this in detail, and concluded that it was due to the pressure resistance on the sensor disk which was proportional to the frictional resistance. Thus, the ratio between C_f and C_{fp} should be constant, as seen in Fig. 3. They also concluded that the ratio of shear stress C_f/C_{f0} was reliable where C_f and C_{f0} were the frictional resistances with and without microbubbles, respectively.

Figure 4 shows the rate of reduction of the frictional resistance C_f/C_{f0} plotted against the mean void ratio α_m, which is expressed by Eq. 3. C_{f1} and C_{f2} are the data from transducers at 0.75 m and 1.25 m from the air injection port, respectively.

$$\alpha_m = \frac{Q_a}{Q_a + Q_w} \tag{3}$$

The experimental conditions are flow velocities of 5, 6, and 7 m/s, and an air injection rate of 0–50 l/min. For each set of experimental conditions, more than 8000 values of frictional resistance were averaged for shear transducers at both upstream and downstream positions. As seen in the figure, the reduction rate is more

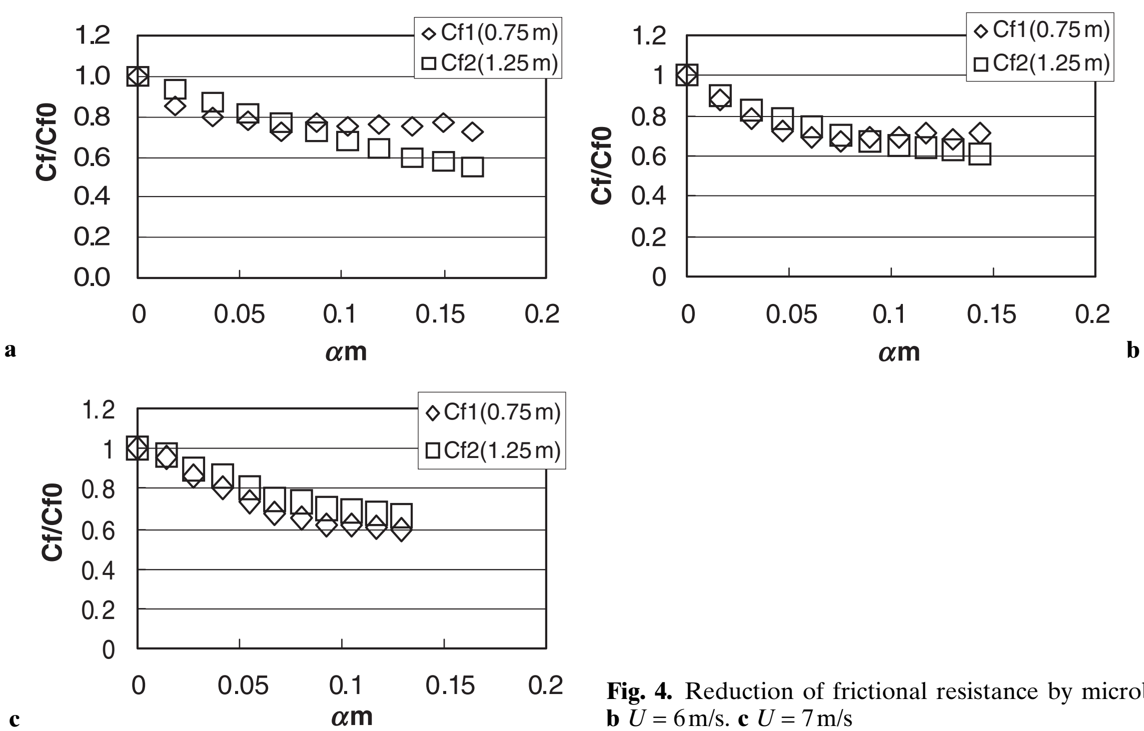

Fig. 4. Reduction of frictional resistance by microbubbles. **a** U = 5 m/s. **b** U = 6 m/s. **c** U = 7 m/s

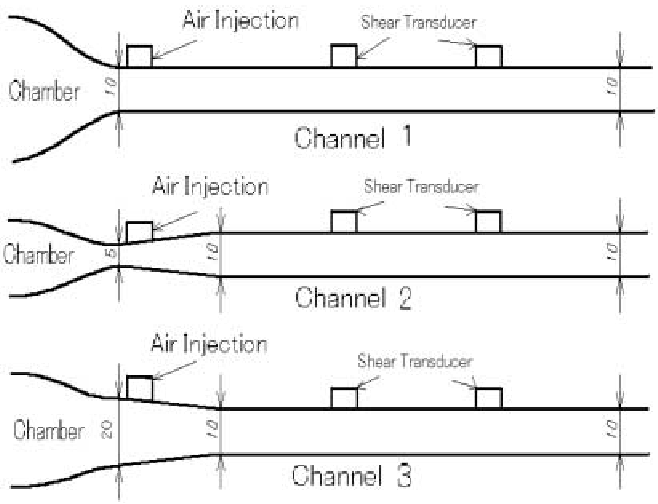

Fig. 5. Change of channel height at the air injection port

than 40% at $\alpha_m = 12\%$. This is in good agreement with the results obtained by Madavan et al.[4] and Kato et al.[6] However, the present results show a difference of about 10% compared with the results we obtained using different experimental apparatus with $h = 15$ mm,[11] and the results of experiments with the same channel by Guin et al.[7]

Measurement of microbubble diameter

The diameter of the microbubbles was changed by using three different channels, as shown in Fig. 5. The diameter of the air bubbles depends mainly on the flow velocity at the position where air injection takes place. All three channels have the same test section height of 10 mm. Channel 1 has an air injection channel height of 10 mm and is the one used for most of the experiment. Channel 2 has an air injection channel height of 5 mm and generates smaller bubbles than channel 1. Channel 3 has an air injection channel height of 20 mm and generates larger bubbles than channel 1.

Figure 6 shows photographs of microbubbles taken from the upper surface of the channel. The upper photograph shows the flow in channel 2, where it was found that the mean microbubble diameter was small. The lower photograph shows the flow in channel 3, where it was found that the mean microbubble diameter was large. Images such as those in Fig. 6 were analyzed using image processing software. Figure 7 shows the distribution of microbubble diameters where the mean void ratio was $\alpha_m = 10\%$ and the flow velocities were 4, 6, and 8 m/s. The distribution resembles a Rayleigh distribution; the thick vertical lines show the mean diameters.

Figure 8 shows the relation between the flow velocity and the mean microbubble diameter. When the main flow velocity is higher, the mean bubble diameter becomes smaller. This tendency corresponds to other experimental results.[7,8] Meng and Uhlman[15] gave the empirical Eq. 4 for the bubble diameter in a boundary layer flow. The tendency in these experiments agrees with Eq. 4.

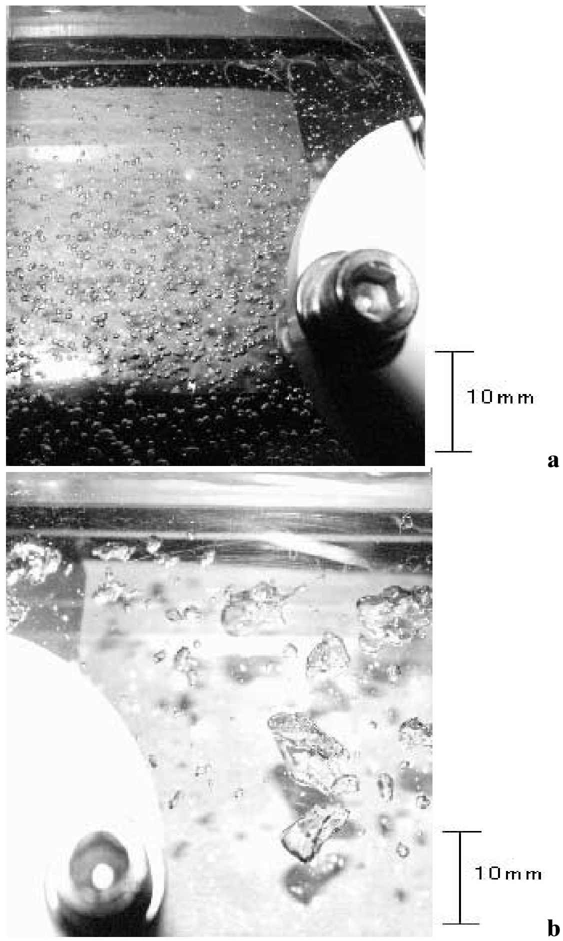

Fig. 6. Photographs of microbubbles in different channels ($U_m = 5$ m/s). **a** Channel 2. **b** Channel 3

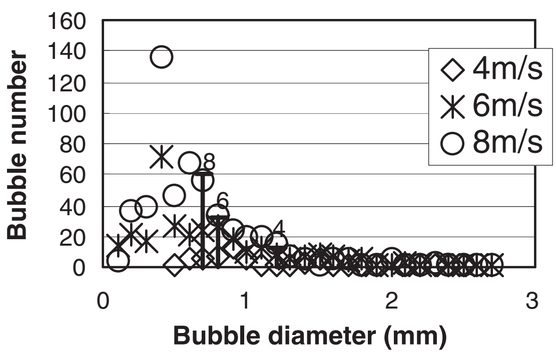

Fig. 7. Distribution of microbubble diameters

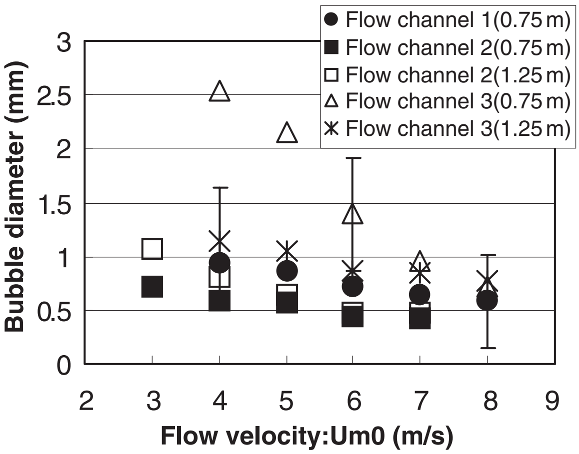

Fig. 8. Effect of main flow velocity on mean microbubble diameter

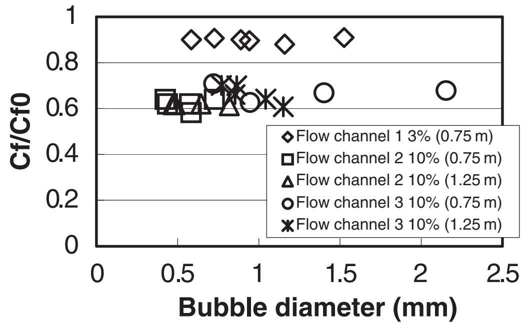

Fig. 9. Effect of mean microbubble diameter on frictional resistance reduction

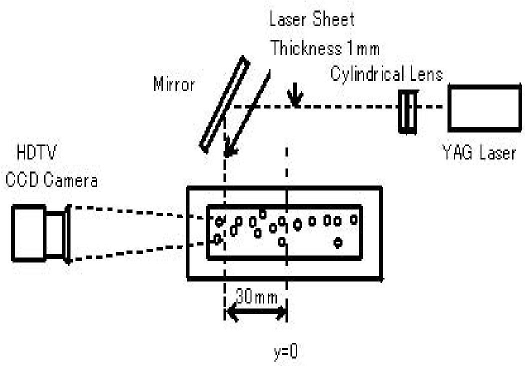

Fig. 10. Measurement of microbubble distribution by the laser light-sheet method

$$\frac{d}{D} = 2.4\sqrt{\frac{Q}{UD^2}} \tag{4}$$

With the same mean void ratio α_m = 10%, and the same flow velocity (3–8 m/s) at the upstream position of 750 mm, the diameter of the microbubbles changed according to which channel was used. However, the bubbles changed their size downstream by splitting into two bubbles and/or by two bubbles merging into one bubble. It seems that the diameter of the bubbles converges to a fixed value depending on the flow velocity at the downstream position. The distance between the two measurement positions was 500 mm, and it was not expected that the microbubble diameters would change greatly in such a short distance. The estimated errors of typical measured values are shown in Fig. 8.

Effect of bubble size on frictional resistance reduction

Figure 9 shows the effect of the mean microbubble diameter on the frictional resistance reduction at α_m = 3% and α_m = 10%. As seen in Fig. 9, even when the average microbubble diameter changed, there was almost no change in the frictional resistance.

Measurement of microbubble distribution

The density of microbubbles near the wall is considered to have a significant influence on frictional resistance reduction. Kakugawa et al.[16] investigated the bubble distribution and its influence on the reduction using an optical set-up. Our measurement system was similar to theirs. As shown in Fig. 10, a laser light sheet illuminated the microbubbles at a distance of 30 mm from the center of the test section where there were no other bubbles to obstruct photography, and there was no influence from the side wall. The thickness of the laser sheet was 1 mm. The microbubbles were photographed from the side.

A straight line was drawn on the photograph parallel to the wall surface at intervals of 0.5 mm, as shown in Fig. 11. The lengths of the line segments that crossed microbubbles were added together, and this value as a percentage of the total length of the segment was considered to be the apparent local void ratio. Since the total of the line segments refers to the largest microbubbles within a laser light sheet of 1 mm thickness, the measured local void ratio should be larger than the true value, and therefore require correction. We adopted a simple correction method. We found the constant correction factor from the fact that the measured average void ratio should be equal to that from the volume of air injected. The slip ratio of microbubbles was estimated to be 0.

Figure 12 shows the corrected distribution of the local void ratio, where the experimental conditions are flow velocities of 6 and 7 m/s, and the mean void ratios α_m are 3% and 9%. Although microbubbles accumulate near the wall because of lift and buoyancy forces, the number of microbubbles decreases in the region nearest to the wall. Our bubble distribution agrees with the results of

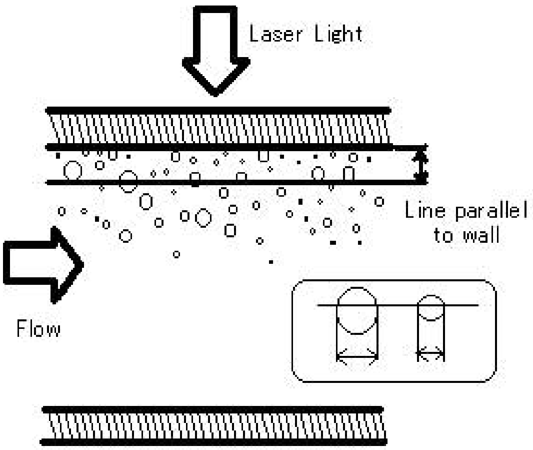

Fig. 11. Apparent void ratio

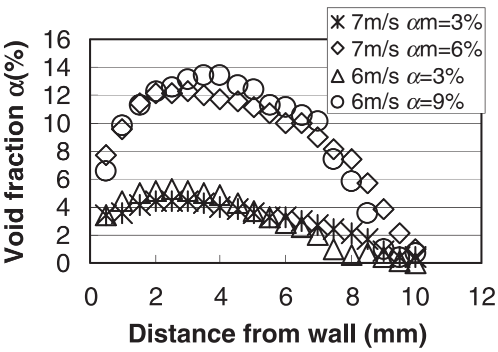

Fig. 12. Local void ratio

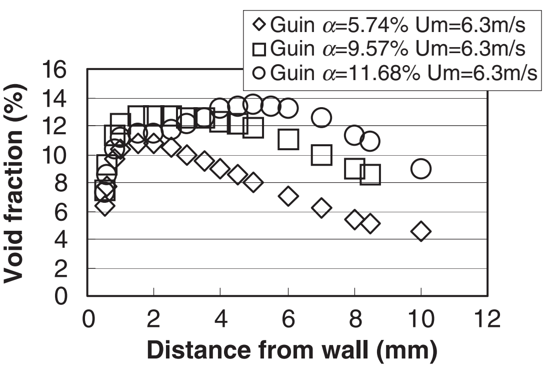

Fig. 13. Local void ratio by Guin et al.[7]

Guin et al. (Fig. 13), which were obtained using the same two-dimensional channel. Our bubble distributions at $\alpha_m = 9\%$ and 3% correspond to $\alpha_m = 11.68\%$ and 5.74%, respectively, from the experiments of Guin et al. It seems that microbubbles gather in the center of the channel when the mean void ratio is large.

The influence of microbubbles near the wall on the reduction of frictional resistance was investigated.

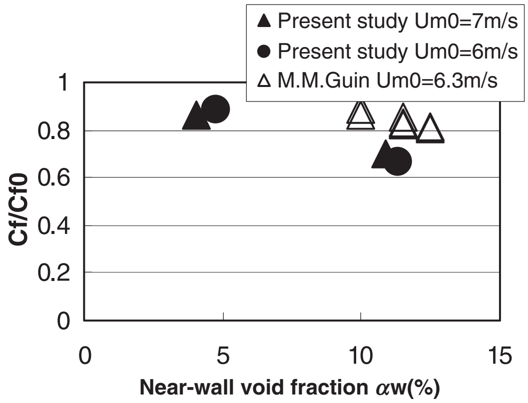

Fig. 14. C_f/C_{f0} vs. near-wall void ratio

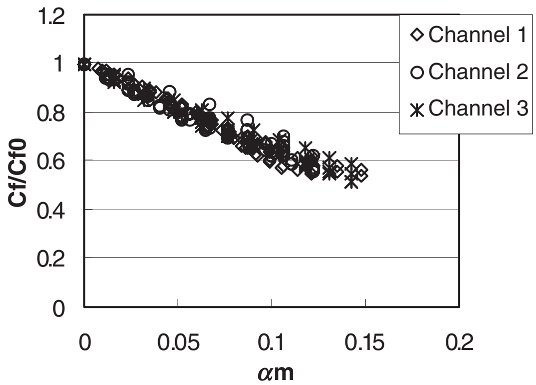

Fig. 15. C_f/C_{f0} vs. mean void ratio

Figure 14 shows the relation between the resistance reduction and the local void ratio near the wall (α_w) (Eq. 5).

$$\alpha_w = \frac{1}{y}\int_0^y \alpha \mathrm{d}y \tag{5}$$

In order to allow a comparison with the results of Guin et al., we defined α_w as the mean void ratio 0–1 mm from the wall. Although the results agree fairly well, the present result shows the effect of microbubbles better than the result of Guin et al.

Considerations

We conducted more than 400 experiments under various conditions. All data on the frictional resistance reduction were well expressed by the mean void ratio, as shown in Fig. 15. At the present stage of this research, we cannot be sure that the only governing factor is the mean void ratio. In spite of a constant void ratio, the void distribution might be changed by factors such as the flow configuration or the turbulence intensity of the flow, which might change the frictional resistance at the wall. In solid–liquid flow and solid–gas flow, it is know that the influence of solid particles on the structure of turbulent flow changes with the diameter of the solid particles.[17] When the diameter is larger than the characteristic length of turbulent flow, the turbulence intensity increases. In contrast, when the solid particles are small, the turbulence intensity decreases due to the presence of the solid particles.

The present findings do not agree with the previous results for solid mixed flow. Within the limits of the experimental results of this research, there was no influence on resistance reduction in spite of large changes in bubble diameter, as seen in Figs. 9 and 15. Further experiments are required, including carrying out turbulence intensity measurements near the wall.

Conclusions

The effect of microbubbles on frictional resistance reduction was examined in a two-dimensional turbulent flow channel, with the main aim of clarify in of the bubble size effect. We changed the diameter of microbubbles by changing the flow velocity at the air injection port. Shear transducers measured the frictional resistance directly, and the diameter of the microbubbles and the bubble distribution were also measured using an optical method.

The following results were obtained.

1. The frictional resistance reduction increased with increasing mean void ratio.
2. Contrary to the result anticipated, there was almost no effect of microbubble diameter on frictional resistance reduction.

Detailed measurements are necessary in the future, including measurements of the turbulence intensity and the local void ratio near the wall.

Acknowledgments. This research was supported by a special research program of Toyo University, SR239 Research Committee of the Shipbuilding Research Association of Japan, and the Research Project on Smart Control of Turbulence. The authors express their sincere gratitude for these supports.

References

1. McCormick ME, Bhattacharyya R (1973) Drag reduction of a submersible hull by electrolysis. Nav Eng J 85:11–16
2. Bogdevich VG, Evseev AR, Malyuga AG, et al (1977) Gas saturation effect on near-wall turbulence characteristics. 2nd International Conference on Drag Reduction, Cambridge. BHRA, pp 25–37
3. Madavan NK, Deutsch S, Merkle CL (1984) Reduction of turbulent skin friction by microbubbles. Phys Fluids 27:356–363
4. Madavan NK, Deutsch S, Merkle CL (1985) Measurements of local skin friction in a microbubble-modified turbulent boundary layer. J Fluid Mech 156:237–256
5. Madavan NK, Deutsch S, Merkle CL (1985) Numerical investigation into the mechanisms of microbubble drag reduction. J Fluids Eng 107:370–377
6. Kato H, Miyanaga M, Yamaguchi H, et al (1995) Frictional drag reduction by injecting bubbly water into a turbulent boundary layer and the effect of plate orientation. In: Serizawa A, Fukano T, Bataille J (eds) Advances in multiphase flow. Elsevier, Amsterdam, pp 85–96
7. Guin MM, Kato H, Yamaguchi H, et al (1996) Reduction of skin friction by microbubbles and its relation with near-wall bubble concentration in a channel. J Mar Sci Technol 1:241–254
8. Kato H, Miura K, Yamaguchi H, et al (1998) Experimental study on the microbubble ejection method for frictional drag reduction. J Mar Sci Technol 3:122–129
9. Kato H, Iwashina T, Yamaguchi H, et al (1999) Effect of microbubbles on the structure of turbulence in a turbulent boundary layer. J Mar Sci Technol 4:155–162
10. Kato H, Iwashina T, Miyanaga M, et al (1999) Effect of microbubble clusters on turbulent flow structure. IUTAM Symposium on Mechanics of Passive and Active Flow Control, pp 255–260
11. Moriguchi Y, Kato H, Kodama Y, et al (2000) Mechanism of frictional resistance reduction by microbubbles (in Japanese). OMF 2000, Takayama, pp 17–22
12. Watanabe O, Masuko A, Shirase Y (1999) Measurements of drag reduction by microbubbles using very long ship models (in Japanese). Soc Nav Archit Jpn 183:53–63
13. Takahashi T, Kakugawa A, Makino M, et al (2000) Introduction of a microbubble experiment using the flat bottom model ship with a length of 50m (in Japanese). 74th National Maritime Research Institute, Research Presentation Lecture Collection No. 52
14. Kodama Y, Kakugawa A, Takahasi T, et al (1999) Experimental study on microbubbles and their applicability to ships for skin friction reduction. Proceedings of the 1st International Symposium on Turbulent Shear Flow Phenomena
15. Meng JCS, Uhlman JS Jr (1989) Microbubble formulation and splitting in a turbulent boundary layer for turbulence reduction. Symposium in Honor of Maurice Holton on his 70th Birthday
16. Kakugawa A, Kawashima H, Takahashi T, et al (1997) The effect of microbubble distributions on drag reduction (in Japanese). Proceedings of the 70th General Meeting of the Ship Research Institute
17. Gore RA, Growe CT (1988) Effect of particle size on modulating turbulent intensity. J Multiphase Flow 15:279–285